

Development of Two Directional DC/DC Converter with Dual-Battery Energy Storage for Hybrid Electric Vehicle System

Drusti J S

Student,

Sri Siddhartha Institute of Technology,
SSAHE ,Tumkur ,

Girish S K

Assistant Professor,

Sri Siddhartha Institute of Technology,
SSAHE , Tumkur.

Abstract-- Present research work aims at developing a bi-directional DC/DC converter (BDC) connecting the main energy storage (ES1), auxiliary energy storage (ES2) and DC bus with Different voltage levels for use in hybrid automotive electrical systems. With bidirectional current regulation, the proposed converter can operate in both boost mode (low voltage dual power supply mode) and buck mode (mains uninterruptible power supply regenerative mode high pressure). In addition, the model can independently manage the current between two low voltage sources (dual low voltage source boost/drop mode). According to the three power transmission methods provided by BDC, circuit layout, operation, steady-state analysis and closed-loop control are introduced. In addition, the proposed converter is validated using simulation results for the 1 kW prototype system. MATLAB / Simulink software is used to perform simulation work.

Keywords-- Bidirectional dc/dc converter, main energy storage, an auxiliary energy storage, MATLAB/Simulink.

I. INTRODUCTION

Bidirectional power flow is not possible with basic dc-dc converters like buck and boost converters (and their variants). The presence of diodes in its construction precludes reverse current flow, resulting in this constraint. In principle, a unidirectional dc-dc converter may be made bidirectional by replacing the diodes in its construction with a programmable switch. Many power-related systems, such as hybrid vehicles, fuel cell vehicles, renewable energy systems, and so on, have found the bidirectional dc-dc converter and energy storage to be a viable alternative. It not only lowers costs and increases efficiency, but it also enhances the system's performance. An auxiliary energy storage battery captures the regenerated energy sent back by the electric machine in electric vehicle applications. Furthermore, a bidirectional dc-dc converter is necessary to take power from the auxiliary battery in order to enhance the high-voltage bus during vehicle starting, acceleration, and hill climbing. Bidirectional dc-dc converters are increasingly being utilised to facilitate power transfer between two dc power sources in either direction due to their capacity to reverse the direction of current flow and therefore power. The multiple-input bidirectional dc-dc converter may be used to integrate diverse types of energy sources in renewable energy applications. This bidirectional dc-dc converter has galvanic isolation between the load and the fuel cell, bidirectional power

flow, voltage matching capabilities, and quick response to transient load demand, among other advantages. Renewable electric power generating systems have recently been developed using clean energy resources such as solar arrays and wind turbines. When the dc bus voltage is low, the bidirectional dc-dc converter is frequently used to transmit solar energy to the capacitive energy source while delivering energy to the load. The majority of contemporary bidirectional dc-dc converters have a circuit configuration like the one shown in the diagram, which is defined by a current or voltage provided on one side.

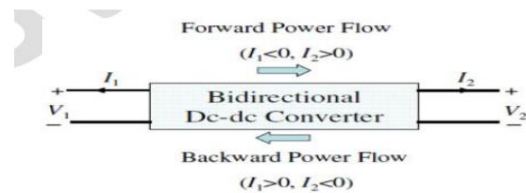


Fig 1: Bidirectional dc-dc converters

The bidirectional dc-dc converter can be classified as buck or boost depending on where the supplementary energy storage is located. Energy storage is put on the high voltage side in the buck type, whereas it is positioned on the low voltage side in the boost type. In bidirectional dc-dc converters, the switch cell must conduct current in both directions to achieve double-sided power flow. Because a double-sided current flow power switch is not accessible, it is commonly accomplished with a unidirectional semiconductor power switch such as a power MOSFET (Metal-Oxide-Semiconductor-Field-Effect Transistor) or IGBT (Insulated Gate Bipolar Transistor) in tandem with a diode. The bidirectional power flow is achieved in buck and boost dc-dc converters by replacing the switch and diode with the double sided current switch cell illustrated below:

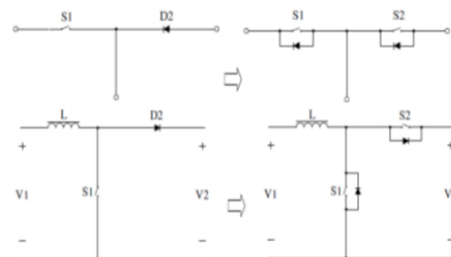


Fig 2: The bidirectional power flow is achieved in buck and boost dc-dc converters by replacing the switch and diode with the double sided current switch cell

II. PROBLEM STATEMENT

A new BDC topology for FCV/HEV power systems that consists of an interleaved voltage-doubler structure and a synchronous buck-boost circuit is proposed. To control the power flow from energy storage devices to motor in motoring mode and from motor to energy storing devices during braking mode.

In addition, the proposed converter can independently control power flow between any two low-voltage sources when in the low-voltage dual-source buck/boost mode. To increase the static voltage gain and thus reduces switch voltage stress, and To generate wide voltage difference between its high- and low-side ports with reasonable duty ratio.

III. Proposed Three-switch Three-port Flyback with Series Power Decoupling Circuit

The proposed BDC topology with dual-battery energy storage is provided below, where V_H , V_{ES1} , and V_{ES2} represent the high-voltage dc-bus voltage, the main energy storage (ES1), and the auxiliary energy storage (ES2) of the system, respectively.

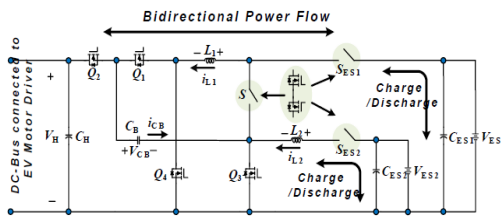


Fig 3: BDC architecture with dual-battery energy storage

Two bidirectional power switches (SES1 and SES2) in the converter structure, are used to switch on or switch off the current loops of ES1 and ES2, respectively. A charge-pump capacitor (CB) is integrated as a voltage divider with four active switches (Q1, Q2, Q3, Q4) and two phase inductors (L1, L2) to improve the static voltage gain between the two low-voltage dual sources (VES1, VES2) and the high-voltage dc bus (VH) in the proposed converter. Furthermore, the additional CB reduces the switch voltage stress of active switches and eliminates the need to operate at an extreme duty ratio. Furthermore, the three bidirectional power switches (S, SES1, SES2) exhibit four-quadrant operation and are adopted to control the power flow between two low-voltage dual sources (VES1, VES2) and to block either positive or negative voltage. This bidirectional power switch is implemented via two metal-oxide-semiconductor field-effect transistors (MOSFETs), pointing in opposite directions, in series connection.

• OPERATION MODES AND ANALYSIS

The conduction statuses of the power devices involved in each operation mode are displayed in following table:

Table 1: The conduction characteristics of such power devices engaged in each operating mode

Operating Modes	ON	OFF	Control Switch	Synchronous Rectifier (SR)
Low-voltage dual-source-powering mode (Accelerating, $\alpha=1, \beta=1$)	SES1, SES2	S	Q3, Q4	Q1, Q2
High-voltage dc-bus energy-regenerating mode (Braking, $\alpha=1, \beta=1$)	SES1, SES2	S	Q1, Q2	Q3, Q4
Low-voltage dual-source buck mode (ES1 to ES2, $\alpha=0, \beta=0$)	SES1, SES2	Q1, Q2, Q4	S	Q1
Low-voltage dual-source boost mode (ES2 to ES1, $\alpha=0, \beta=0$)	SES1, SES2	Q1, Q2, Q4	Q1	S
System shutdown	-	SES1, SES2, Q1, Q2, Q3, Q4	-	-

• Low-Voltage Dual-Source-Powering Mode

The circuit schematic for the proposed converter under the low-voltage dual-source-powering mode is provided below:

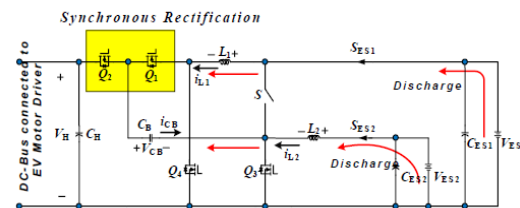


Fig 4: Low voltage dual source powering mode

In this, the switch S is turned off, and the switches (SES1, SES2) are turned on, and the two low-voltage dual sources (VES1, VES2) are supplying the energy to the dc-bus and loads. In this mode, the low-side switches Q3 and Q4 are actively switching at a phase-shift angle of 180°, and the high-side switches Q1 and Q2 function as the synchronous rectifier (SR).

Some key waveforms of the proposed converter are depicted in following graphs:

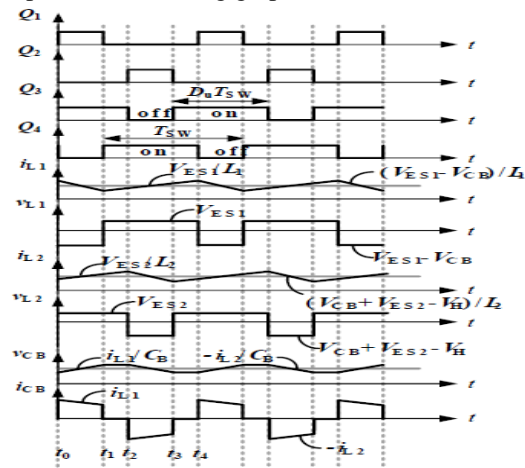


Fig 5: converter's important waveforms

When the duty ratio is larger than 50%, four circuit states are possible

State 1 [$t_0 < t < t_1$]: During this state, the interval time is $(1-D_u)T_{sw}$, switches Q1, Q3 are turned on, and switches Q2, Q4 are turned off.

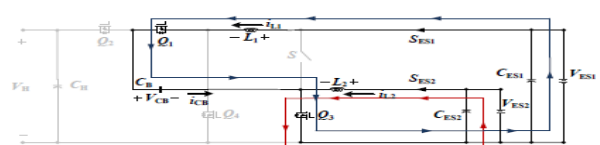


Fig 6: Low voltage dual source powering mode(State-1)

The voltage across L1 is the difference between the low-side voltage VES1 and the charge-pump voltage (VCB), and hence i_{L1} decreases linearly from the initial value. In addition, inductor L2 is charged by the energy source VES2, thereby generating a linear increase in the inductor current. The voltages across inductors L1 and L2 can be denoted as

$$L_1 \frac{di_{L1}}{dt} = V_{ES2} - V_{CB}$$

$$L_2 \frac{di_{L2}}{dt} = V_{ES2}$$

State 2 [$t1 < t < t2$]: During this state, the interval time is $(Du-0.5)Tsw$; switches Q3 and Q4 are turned on; and switches Q1 and Q2 are turned off.

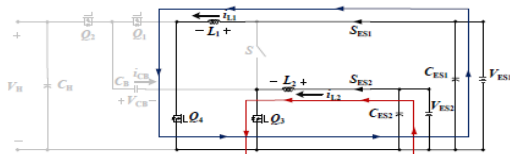


Fig 7:Low voltage dual source powering mode(State-2)

The low-side voltages VES1 and VES2 are located between inductors L1 and L2, respectively, thereby linearly increasing the inductor currents, and initiating energy to storage. The voltages across inductors L1 and L2 under state 2 can be denoted as

$$L_1 \frac{di_{L1}}{dt} = V_{ES1}$$

$$L_2 \frac{di_{L2}}{dt} = V_{ES2}$$

State 3 [$t2 < t < t3$]: During this state, the interval time is $(1-Du)Tsw$; switches Q1 and Q3 are turned on, whereas switches Q2 and Q4 are turned off.

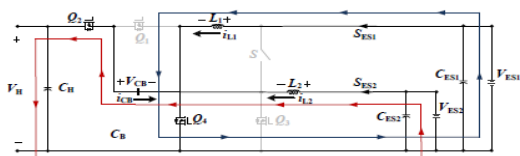


Fig 8:Low voltage dual source powering mode(State-3)

The voltages across inductors L1 and L2 can be denoted as

$$L_1 \frac{di_{L1}}{dt} = V_{ES1}$$

$$L_2 \frac{di_{L2}}{dt} = V_{CB} + V_{ES2} - V_H$$

State 4 [$t3 < t < t4$]: During this state, the interval time is $(Du-0.5)Tsw$; switches Q3 and Q4 are turned on, and switches Q1 and Q2 are turned off.

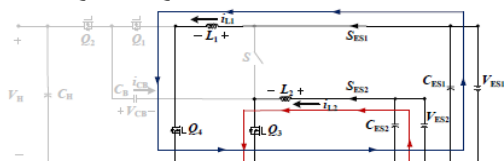


Fig 9:Low voltage dual source powering mode(State-4)

The voltages across inductors L1 and L2 can be denoted as

$$L_1 \frac{di_{L1}}{dt} = V_{ES1}$$

$$L_2 \frac{di_{L2}}{dt} = V_{ES2}$$

• **High-Voltage DC-Bus Energy-Regenerating Mode**

In this mode, the kinetic energy stored in the motor drive is fed back to the source during regenerative braking operation. The regenerative power can be much higher than what the battery can absorb. Consequently, the excess energy is used to charge the energy storage device. The circuit schematic of the BDC under the high-voltage dc bus energy-regenerating mode

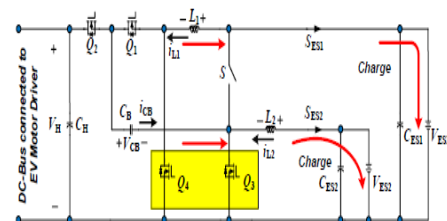


Fig 10: high-voltage dc bus energy-regenerating mode.

In this, the current in the inductors is controlled by the active switches Q1 and Q2, which have a phase-shift angle of 180° and thereby direct the flow away from the dc-bus and toward the dual energy storage devices; the switches Q3 and Q4 function as the SR to improve the conversion efficiency. Some key waveforms of the proposed converter are depicted in following graphs:

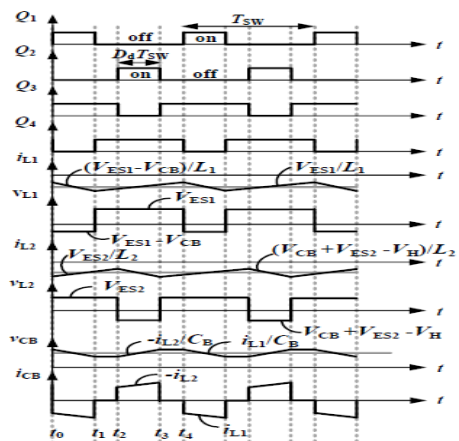


Fig 11: converter's important waveforms

State 1 [$t0 < t < t1$]: During this state, the interval time is $DdTsw$; switches Q1 and Q3 are turned on, and switches Q2 and Q4 are turned off. The voltage across L1 is the difference between the low-side voltage VES1 and the charge-pump voltage VCB; hence, the inductor current i_{L1} decreases linearly from the initial value. In addition, inductor L2 is charged by the energy source VES2, which also contributes to the linear increase in the inductor current.

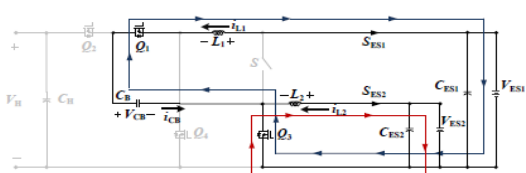


Fig 12: high-voltage dc bus energy-regenerating mode(State-1)

The voltages across inductors L1 and L2 can be denoted as

$$L_1 \frac{di_{L1}}{dt} = V_{ES1} - V_{CB}$$

$$L_2 \frac{di_{L2}}{dt} = V_{ES2}$$

State 2 [t1 < t < t2]: During this state, the interval time is (0.5-Dd)Tsw; switches Q3 and Q4 are turned on, and switches Q1 and Q2 are turned off.

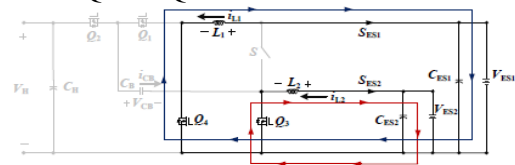


Fig 13: high-voltage dc bus energy-regenerating mode(State-2)

The voltages across inductors L1 and L2 are the positive the low-side voltages VES1 and VES2, respectively; hence, inductor currents iL1 and iL2 increase linearly. These voltages can be denoted as

$$L_1 \frac{di_{L1}}{dt} = V_{ES1}$$

$$L_2 \frac{di_{L2}}{dt} = V_{ES2}$$

State 3 [t2 < t < t3]: During this state, the interval time is DdTsw; switches Q1 and Q3 are turned off, and switches Q2 and Q4 are turned on.

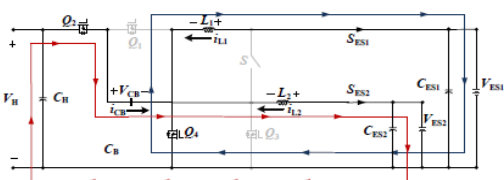


Fig 14: high-voltage dc bus energy-regenerating mode(State-3)

The voltage across L1 is the positive low-side voltage VES1 and hence iL1 increases linearly from the initial value. Moreover, the voltage across L2 is the difference of the high-side voltage V_H, the charge-pump voltage V_{CB}, and the low-side voltage VES2, and its level is negative. The voltages across inductors L1 and L2 can be denoted as

$$L_1 \frac{di_{L1}}{dt} = V_{ES1}$$

$$L_2 \frac{di_{L2}}{dt} = V_{ES2} + V_{CB} - V_H$$

State 4 [t3 < t < t4]: During this state, the interval time is (0.5-Dd)Tsw; switches Q3 and Q4 are turned on, and switches Q1 and Q2 are turned off.

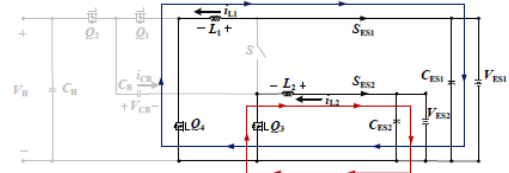


Fig 15: high-voltage dc bus energy-regenerating mode(State-4)

The voltages across inductors L1 and L2 can be denoted as

$$L_1 \frac{di_{L1}}{dt} = V_{ES1}$$

$$L_2 \frac{di_{L2}}{dt} = V_{ES2}$$

• **Low-Voltage Dual-Source Buck/Boost Mode**

The circuit schematic for this mode, which involves the transfer of energy stored in the main energy storage to the auxiliary energy storage and vice versa is shown below:

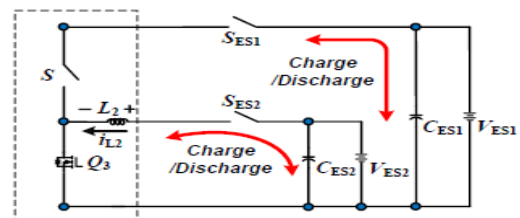


Fig 16: Low-Voltage Dual-Source Buck/Boost Mode

Therein, the topology is converted into a single-leg bidirectional buck-boost converter. When the duty cycle of the active bidirectional switch S is controlled, the buck converter channels power from main energy storage to the auxiliary energy storage. By contrast, when the duty cycle of switch Q3 is controlled, power flows from the auxiliary energy storage to main energy storage, indicating that the converter is operating in boost mode.

• **CONTROL STRATEGY OF PROPOSED CONVERTER**

Block diagram of the proposed converter is provided below:

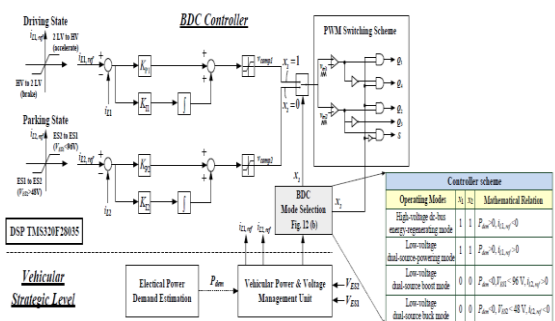


Fig 17:Control strategy of proposed converter

In FCV/HEV power systems, the dc-bus voltage of the driving inverter is regulated and powered by the FC stack through a dc-dc converter. Hence, instead of controlling the converter output voltage of each operation mode, the inductor current iL1 or iL2 is detected and

compared with the reference current to control the power flow. In the converter control structure, the vehicular energy and power and voltage management unit selects the BDC mode according to the operating conditions of the vehicle, such as power demand of different driving state (Pdem) and the dual-source voltages (VES1, VES2). It then selects the appropriate current references $i_{L1,ref}$ or $i_{L2,ref}$ that can control the active switches (S, Q1~Q4) with proportional integral (PI) or more advanced methods. Notably, in spite of it is not easy to choose the optimal parameter of PI controller, the advantages of zero steady-state error and capability of noise filtering, making PI control the most widely used industry algorithm. Furthermore, two switch selector (x1, x2) of BDC controller can be defined for various operating modes. The pulsed-width-modulation (PWM) switching scheme converts the duty cycle determined by different switch selector statuses into gate control signals for the power switches.

The procedure of mode switching is shown in the following flowchart:

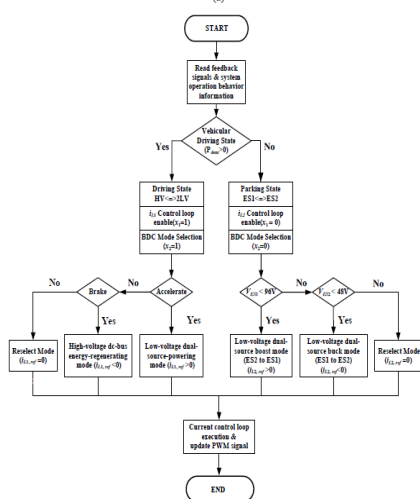


Fig 18: The phase shifting method is depicted

First of all, when vehicle is in driving state ($P_{dem} > 0$), the controller is i_{L1} control loop ($x_1=1$), and the controlled switches (vehicle is accelerating ($i_{L1,ref} > 0$, HV to 2 LV) or braking ($i_{L1,ref} < 0$, 2 LV to HV)). If neither of the two situations, it will execute reselect mode to process the next judgement of mode switching. Additionally, when vehicle is in parking state ($P_{dem} < 0$), the controller is i_{L2} control loop ($x_1=0$), and controlled switches. In this state, the judgement of mode switching depends on the voltage of VES1 (96 V) and VES2 (48 V). If $VES1 < 96$ V, the mode is low-voltage dual-source boost mode ($i_{L2,ref} > 0$, VES2 to VES1). When $VES2 < 48$ V, the mode is low-voltage dual-source buck mode ($i_{L2,ref} < 0$, VES1 to VES2). If both situations do not be satisfied, it executes reselect mode to process the next judgment of mode switching. Only two closed-loop controllers were developed to control the four power flow conditions based on the average model of the proposed converter.

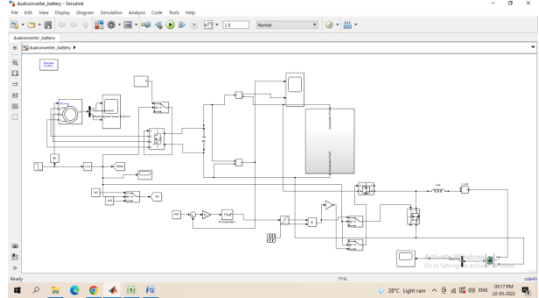
IV. Simulation Setup & Results

The key circuit parameters and their values are listed in the following table

Table I. Simulation Parameters

Specifications	
ES1 voltage	V_{ES1} : 96 V
ES2 voltage	V_{ES2} : 48 V
DC-bus voltage	V_H : 430 V
Output power	P_o : 1 kW
Switching frequency	f_{sw} : 40 kHz

The simulation circuit for the hybrid electric vehicle with dual converter is provided below:

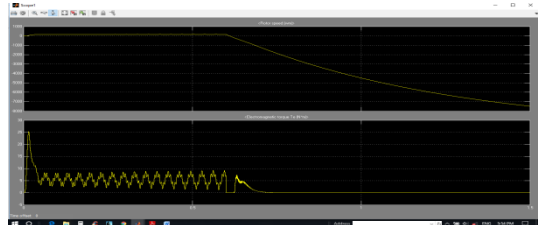


The driving mode and braking mode command signal is provided in the following graph:



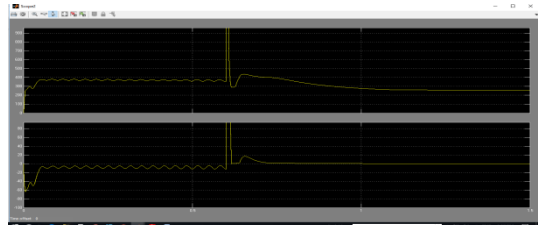
The driving mode occurs when the command signal is HIGH and braking mode occurs when the command signal is LOW.

The speed and torque graph of the induction motor is provided below:



The speed is positive during driving mode and when braking occurs it reduces further below to zero. In practical when it is zero, mechanical brake acts and stops the vehicle.

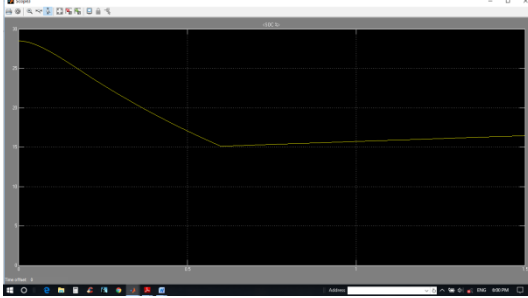
The DC bus voltage and current is provided below:



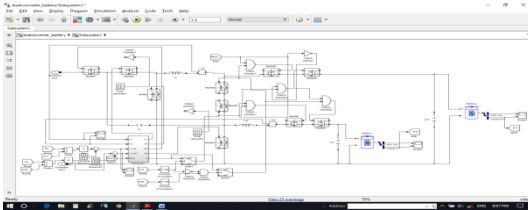
When braking occurs, the current flow direction is reversed as the energy from induction motor windings is recovered and can be used to charge the batteries. After few instance of time, the current is reduced and reaches zero as there is no more energy in the motor windings.

The auxiliary energy storage device used in this system is super capacitor. The super capacitor gets charged from fuel cell as the induction motor is stopped. The

%SOC of super capacitor is provided in the following graph:

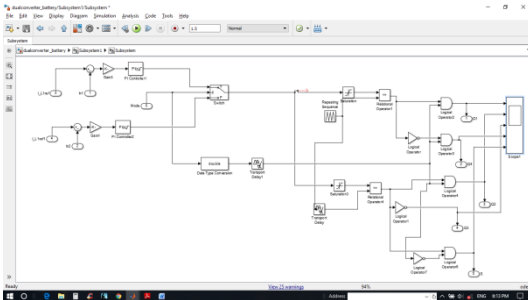


The dual converter simulation circuit is provided below:

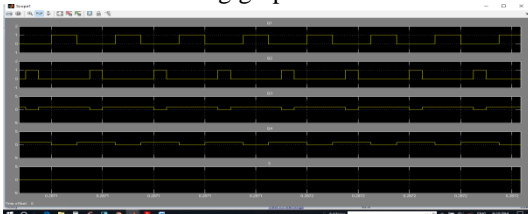


In this, we have two batteries, one is high voltage end and other is low voltage end. The battery will be discharged during motoring mode and gets charged during braking mode. When the energy stored in motor windings are recovered, then the battery having low amount of %SOC can be get charged by the other battery.

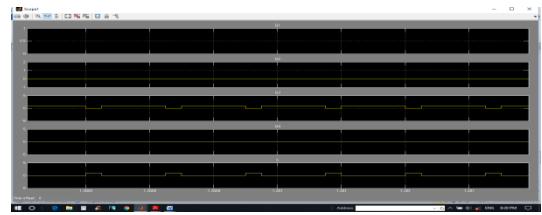
The control circuit for the dual converter is provided below:



In this PI controller is used for both motoring and braking control loops. The duty ratio will be provided by PI controllers which can be compared with high frequency carrier signals to get the gating pulses. The gating pulses are shown in the following graph:

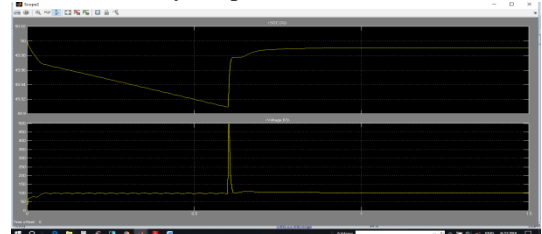


The above pulses are for motoring mode. When self charging/discharging of batteries occurs due to low amount of %SOC in any of the batteries occurs, and then the pulses will be as follows:



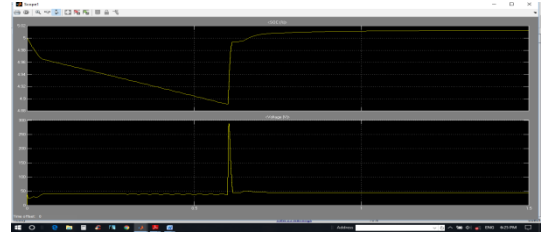
In this only Q3 and S switches will operate. All other switches will be turned OFF.

The %SOC of battery1 is provided below:



In this the battery will be discharged and when braking occurs the energy retrieved from motor is used to charge the battery.

Similarly, the %SOC of second battery is provided below:



V. CONCLUSION

A new BDC topology was presented to interface dual battery energy sources and high-voltage dc bus of different voltage levels. The circuit configuration, operation principles, analyses, and static voltage gains of the proposed BDC were discussed on the basis of different modes of power transfer. Simulation waveforms for a 1 kW prototype system highlighted the performance and feasibility of this proposed BDC topology. The results demonstrate that the proposed BDC can be successfully applied in FC/HEV systems to produce hybrid power architecture.

REFERENCES

- [1] M. Ehsani, K. M. Rahman, and H. A. Toliyat, "Propulsion system design of electric and hybrid vehicles," IEEE Transactions on industrial electronics, vol. 44, no. 1, pp. 19-27, 1997.
- [2] A. Emadi, K. Rajashekara, S. S. Williamson, and S. M. Lukic, "Topological overview of hybrid electric and fuel cell vehicular power system architectures and configurations," IEEE Transactions on Vehicular Technology, vol. 54, no. 3, pp. 763-770, 2005.
- [3] A. Emadi, S. S. Williamson, and A. Khaligh, "Power electronics intensive solutions for advanced electric, hybrid electric, and fuel cell vehicular power systems," IEEE Transactions on Power Electronics, vol. 21, no. 3, pp. 567-577, 2006.
- [4] E. Schaltz, A. Khaligh, and P. O. Rasmussen, "Influence of battery/ultracapacitor energy-storage sizing on battery lifetime in a fuel cell hybrid electric vehicle," IEEE Transactions on Vehicular Technology, vol. 58, no. 8, pp. 3882-3891, 2009.
- [5] P. Thounthong, V. Chunkag, P. Sethakul, B. Davat, and M. Hinaje, "Comparative study of fuel-cell vehicle hybridization with battery or supercapacitor storage device," IEEE transactions on vehicular technology, vol. 58, no. 8, pp. 3892-3904, 2009.

- [6] C. C. Chan, A. Bouscayrol, and K. Chen, "Electric, hybrid, and fuel-cell vehicles: Architectures and modeling," IEEE transactions on vehicular technology, vol. 59, no. 2, pp. 589-598, 2010.
- [7] A. Khaligh and Z. Li, "Battery, ultracapacitor, fuel cell, and hybrid energy storage systems for electric, hybrid electric, fuel cell, and plug-in hybrid electric vehicles: State of the art," IEEE transactions on Vehicular Technology, vol. 59, no. 6, pp. 2806-2814, 2010.
- [8] K. Rajashekhara, "Present status and future trends in electric vehicle propulsion technologies," IEEE Journal of Emerging and Selected Topics in Power Electronics, vol. 1, no. 1, pp. 3-10, 2013.
- [9] C.-M. Lai, Y.-C. Lin, and D. Lee, "Study and implementation of a two-phase interleaved bidirectional DC/DC converter for vehicle and dc-microgrid systems," Energies, vol. 8, no. 9, pp. 9969-9991, 2015.
- [10] C.-M. Lai, "Development of a novel bidirectional DC/DC converter topology with high voltage conversion ratio for electric vehicles and DC-microgrids," Energies, vol. 9, no. 6, p. 410, 2016.